Chapter 3

3D imaging of Plant cells Using Two-beam Off-axis Digital Holographic Interference Microscope

3.1 Introduction

A standard bright field microscope can provide only low contrast 2D profiles of cells and other micro-objects, which are trans-illuminated by visible electromagnetic radiation [55, 98]. In most of the cases use of bright field microscope requires staining of the object for improving image contrast. These microscopes are unable to provide any information on the cell morphology directly. As discussed in Chapter 1, off-axis hologram recording configuration is an imaging modality providing high contrast images of low absorbing objects. They can also provide 3D image of the entire object from a single hologram [20, 22, 25, 26, 27, 30, 31, 33, 34, 35, 36, 37, 38, 39, 40, 48, 49, 50, 69, 70, 78, 99, 100, 101]. This aspect makes this technique suitable not only for mapping the thickness profile of cells (cell morphology) but also for measurement of its thickness change with time (time evolving cell morphology). It will be interesting to apply Digital Holographic Interference Microscope (DHIM) in 3D imaging of cells for studying their time evolution, without the aid of labelling or tagging agents [20, 22, 25, 26, 27, 30, 31, 33, 34, 35, 36, 37, 38, 39, 40, 48, 49, 50, 69, 70, 78, 99, 100, 101]. A two-beam off-axis DHIM in

Mach-Zehnder configuration (MZ-DHIM) [88] is ideal for investigating cells in the transmission mode ensuring separation of the three terms at the reconstruction plane [20, 22, 25, 26, 27, 30, 31, 33, 34, 35, 36, 37, 38, 39, 40, 70, 78, 99, 100, 101].

In this chapter the application of DHIM for investigation and quantification of plant cells is described. Plants rely on osmosis for proper movement of water and minerals which are absorbed by the roots and move up the plants through the xylem [102, 103]. A plant cell has high water pressure and act as the plant supportive structure, responsible for giving it its shape. Plant cell contain a vacuole that stores food, water and wastes. With adequate supply of water it makes the cell turgid and when kept in hypertonic solution, water exits the cell and cell becomes shriveled. Quantitative study of osmosis in the plant cell can be useful in area of plant biology [102]. It will be interesting to investigate these mechanisms using DHIM and quantify them. In the first set of experiments, plant cells were imaged and quantified using this microscope [100, 101]. Plant cells are eukaryotic cells, which contain nucleus, cell wall, vacuole and other organelles. Various parameters are measured for cellular and subcellular organelles. Texture and crispness of fruits and vegetables is partially due to osmosis and diffusion. When preservatives are applied, it creates higher ion concentration at the surface than that exists inside the cells and water permeates through the cell walls to equalize this concentration difference. So the cells lose turgor pressure and begin to collapse. This means that the texture becomes softer and less crisp. The effect of preservative treatment on plant cells, applying sugar solution to the onion cells were investigated using DHIM, which showed the effect of osmosis in these cells as well as texture change in the cells. Cells in various conditions such as germinated onion cells were also investigated and dynamic and static parameters of these cells were extracted and used to study their bio-physical properties. It should be noted that quantitative measurements were done without any staining of biological cells, just by imaging the phase variation of light beam passing through it [100, 101]. Variation in refractive index change and thickness of the specimen due to internal structure and cell morphology introduce phase change in the object beam, thus a modulation of the holographic pattern. Cell morphology is extracted from these modulated hologram (interference) patterns [69, 99].

3.2 Mach-Zehnder interferometer based off-axis digital holographic microscope

Best way to construct an off-axis DHIM is to split the output from the source into two and use one of them to illuminate the object and other as the reference. These two beams travel along different paths. This could be achieved by employing either Michelson interferometr geometry [17, 18, 76, 104] or Mach-Zehnder interferometer geometry [20, 22, 25, 26, 27, 30, 31, 33, 34, 35, 36, 37, 38, 39, 40, 48, 49, 50, 78, 100, 101]. But for working in transmission mode Mach-Zehnder geometry is ideal. Fig.3.1 shows the schematic of the employed DHIM setup in transmission mode [30, 34, 35, 36, 40, 78, 100, 101].

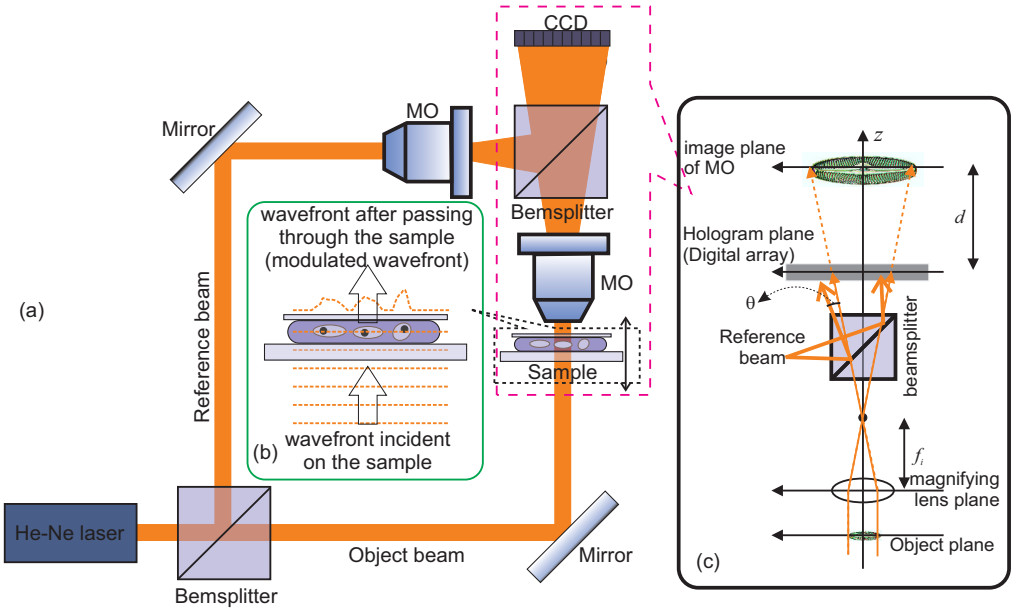

Figure 3.1: (a) Off-axis two-beam DHIM using Mach-Zehnder interferometer geometry. Object beam trans-illuminates the object. Two microscope objective (MO) lenses are used in the setup. Sample is mounted on a translation stage for focusing. (b) Wavefront passing through the object gets modulated because of the spatially varying optical path length distribution of the cells. (c) Object and reference beams are combined by a beamsplitter and allowed to interfere at the detector plane at an angle creating the off-axis geometry. Image plane of the magnifying lens is situated either at the detector plane or very near to it.

Fig.3.2 shows the photograph of the setup whose schematic is shown in Fig.3.1. different parts of the setup are labelled.

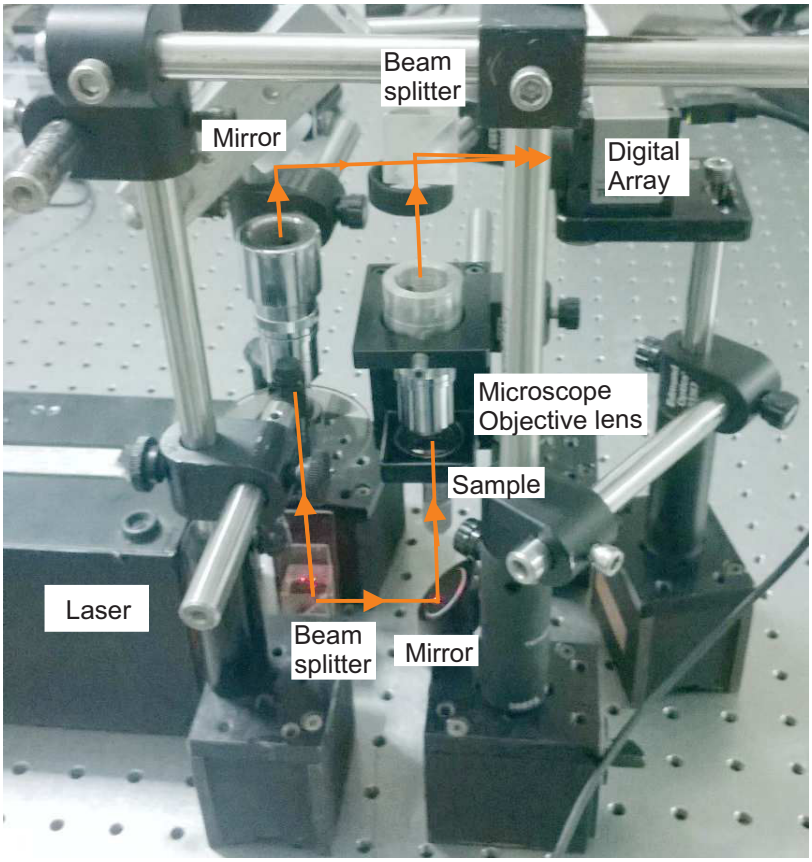

Figure 3.2: Photograph of the table-top arrangement of MZ-DHIM

In the experiments with plant cells, low power He-Ne laser (max output power - 2mW, wavelength 611.9nm, random-linearly polarized) is used as the source to construct a vertical DHIM. Also in these experiments, no spatial filtering is employed to clean the source beam (most of the unwanted phase values will get nullified when the phase subtraction is performed to extract the object phase information). Beam from the source is split using a non-polarizing cube beam splitter (25mm×25mm×25mm). Source light reflected by the beamsplitter beam acts as the reference beam. Light

transmitted by the beamsplitter is allowed to pass through the object under investigation (cells). The object is mounted on a translation stage of 10μm resolution for focusing. The object is magnified using a microscope objective (MO) lens of appropriate magnification and numerical aperture. To match the curvatures of the object and reference wavefronts at the detector plane, an objective of the same magnification and numerical aperture as the one used for magnification of the object is introduced in the reference arm of the setup [104]. Object and the reference beam were made to superpose and create interference patterns (holograms) at the detector plane using a second cube beamsplitter (Coupling the beams also requires a pair of mirrors as shown in Fig.3.1). This beamsplitter is adjusted to introduce a small angle (θ) between the interfering object and reference beams so as to create the off-axis geometry. In most of the experiments, the detector is located at the image plane of the objective lens. In the case of plant cells, most of the experiments, a CCD sensor with 8-bit dynamic range and 4.65μm pixel pitch acted as the hologram recording medium. The beam ratios were adjusted using neutral density filters for high contrast interference fringes. For each set of object holograms a background hologram which does not contain the object (cells) in the field of view but with the background (medium surrounding the cells) present in the field of view is also recorded for phase comparisons (phase subtractions).

Recorded holograms are reconstructed numerically by simulating the diffraction of the reference beam from the microstructures of the interference patterns (this is detailed in section 2.4 of Chapter 2). Briefly it involves the use of angular spectrum approach towards scalar diffraction theory, which describes the propagation of wavefronts between two parallel planes. Since the digitally recorded holograms are discrete in nature (finite pixel and array size), a discrete form of the diffraction integral is used.

3.3 Three dimensional imaging capability of MZ-DHIM

Before studies on plant cells were carried out, the MZ-DHIM setup is used to image a series of known objects to determine, whether it is can be used for high contrast phase imaging as well as to check whether it is suitable for accurate reconstructions

of 3D images of known objects. For testing the phase contrast imaging capability and resolution of the setup (resolution, of course, depends on the numerical aperture of the magnifying lens), an 8-form diatom test slide is used as the sample [98]. A commercial grade 40X, NA=0.65 microscope objective lens (Edmund Optics) is used for magnifying the objects. Holograms were recorded by an 8-bit dynamic range CCD array with 4.65μm pixel pitch (Thorlabs DCU223). For every set of object hologram a background hologram is also recorded. Fig.3.3a and 3.3b shows the recorded object hologram (Surirella Gemma) and background holograms respectively. Intensity profile of the object is obtained by numerically reconstructing the hologram (Fig.3.3a) and using the retrieved complex amplitude distribution in Eqn.(2.5.3). Reconstructed intensity profile is shown in Fig.3.4a. Phase contrast image is obtained from the reconstruct complex amplitude distributions of the object and reference/background holograms and using Eqn.(2.5.1). Quantitative phase image of the object after phase subtraction is shown in Fig.3.4b. This phase difference distribution is used along with Eqn.(2.5.3) to reconstruct the optical thickness profile of the objet shown in Fig.3.4c.

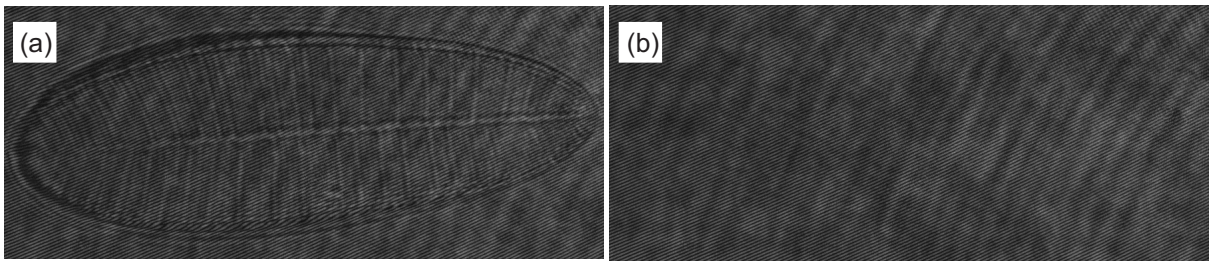

Figure 3.3: (a) Object hologram recorded with of 8-form diatom test slide (Surirella Gemma). (b) Background hologram for the same.

3.4 Spatial phase stability of MZ-DHIM

The ability to image thickness variations (variation in the axial direction) with fine details from a single hologram is the biggest advantage of quantitative phase imaging using DHIM. The minimum detectable phase variation in the axial direction (axial resolution) is determined by the spatial phase stability of the setup (lateral resolution

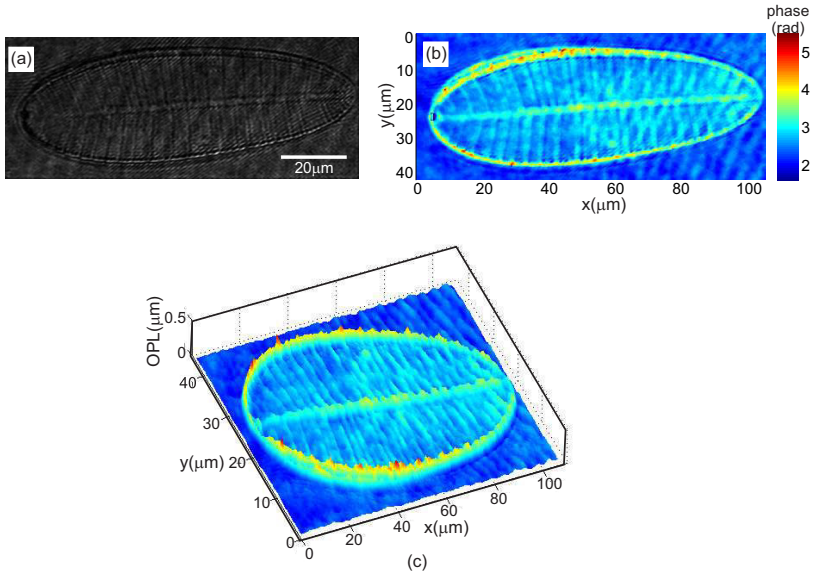

Figure 3.4: (a) Retrieved object intensity distribution at the image plane. (b) Phase difference (quantitative phase image of the object) obtained after phase unwrapping. (c) Optical thickness distribution of the object.

is determined by the numerical aperture of the imaging lens). This depends upon the stability (spatial) of the beam illuminating the object as well as on the spatial phase variations introduced by the optical elements of the microscope as well as on the uniformity (detector quality) of recorded intensity pattern (hologram) by the detector. Since the phase due to the beam profile and that introduced by the optical elements remains same between the object and background holograms, subtraction of background phase from object phase nullify most of the unwanted spatial phase variations [36]. Spatial stability of the setup is determined from the phase difference obtained using two holograms recorded with the setup at two time instances, without any object in the field of view. Fig.3.5a shows the continuous phase distribution after phase subtraction of the holograms recorded with a time gap of 10 minutes. Average of standard deviation of the phase variation at different regions in the phase map provides the spatial phase stability of the microscope [36]. Fig.3.5b shows the three dimensional rendering of phase distribution inside the region shown in Fig.3.5a. This shows the variation in phase distribution even after phase subtraction. Ideally

the phase profile should have been flat (zero standard deviation). Fig.3.5c shows the histogram of the phase variation inside the rectangle in Fig.3.5a. The standard deviation of these values serves as the spatial phase stability of the microscope [36].

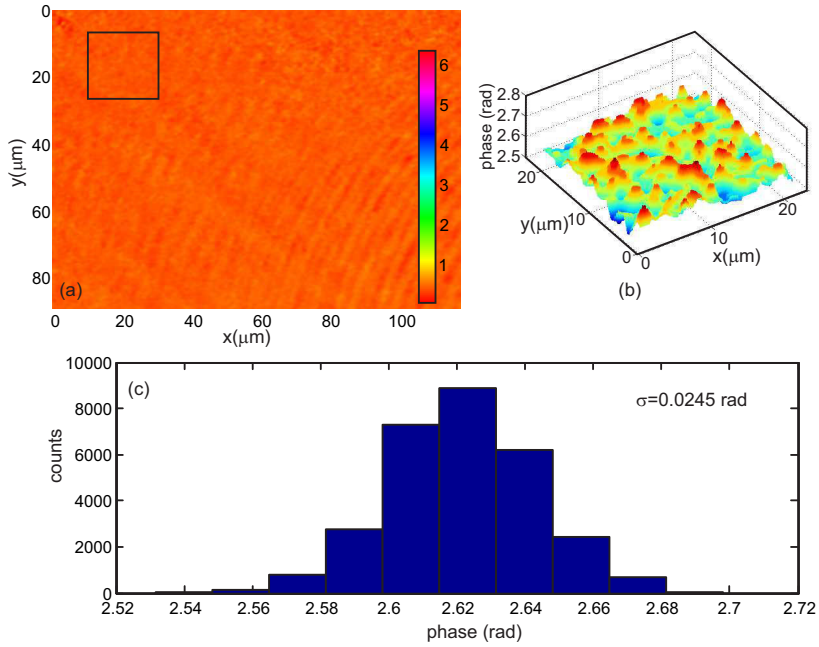

Figure 3.5: Spatial phase stability. (a) Phase difference profile without any object in the field of view. (b) Three dimensional rendering of the phase variation in the rectangular area shown in Fig.3.5a. (c) Histogram of the phase profile inside the rectangular area.

Average of the standard deviations of the spatial phase variation is used as the measurement of spatial phase stability. The obtained spatial phase stability (axial phase resolution) can be converted to a spatial optical thickness resolution using Eqn.(2.5.3). The obtained value for this configuration is 2.37nm.

3.5 Temporal phase stability of MZ-DHIM

Main aim of the study as mentioned in the introduction section is to measure various cell parameters based on its 3D profile as a function of time. This requires studying the cells over a period of time and the minimum variation in the reconstructed phase profile measurable with respect to time decides the temporal resolution (in

the measurement of thickness) of the system. This is an important parameter in measuring the time evolving thickness profiles of cells with accuracy [105]. Temporal phase stability depends upon many factors. This includes temporal stability of the source (variation of source intensity and drift in source wavelength), temporal stability of the microscope structure and temporal stability of the sensor recording the holograms. Variation in the source output over time will result in the change of interference patterns with time as the spatial frequency of interference pattern depends upon its wavelength and the spatial stability (stability of phase in space) depends upon its intensity profile. Source stability can be increased by a frequency stabilized laser. For a given source, the temporal stability of the microscope structure (which includes 2 beamsplitters, two mirrors and MOs as well as translation stage for the sample) become very important in increasing the temporal phase stability. Since in MZ-DHIM, object and reference beam travel along two different paths (Fig.3.1), they are likely to pick up uncorrelated phase oscillations even when vibration isolation mechanisms are employed. This will reduce the temporal phase stability of the setup. For a given source stability and structural stability, the phase stability of the system may still be deteriorated by the detector array. For example in the case of CMOS array, the spatial and temporal variation in intensity will be higher compared to a CCD array. So the use of a CCD array to record holograms, may increase the phase temporal stability, but at the price of increase in the cost and reduction in the maximum sampling rate possible. Temporal phase stability is obtained from a series of holograms recorded with a blank microscope slide as the object. Phase is recovered by numerical reconstruction of each hologram. Standard deviation (along the time axis) at a fixed space point provides the phase fluctuation at that point. Average of the standard deviations (along the time axis) over the entire field of view provides the temporal phase stability of the microscope. For determination of phase fluctuations holograms are recorded at the rate of 20Hz (full field of view) for 1 minute (1200 holograms) and the phase reconstructions were done. This is then used to determine the standard deviation of phase change at each spatial location leading to determination of temporal phase stability. Fig.3.6a shows the standard deviation (at each spatial point) of phase change for a region consisting of 300×300 pixels (field of view

of approximately $35\mu m \times 35\mu m$). The mean of these values acts as the measure of temporal phase stability. Fig.3.6b shows the time variation in phase along the points shown in Fig.3.6a. Histogram of the fluctuations for the region analyzed is shown in Fig.3.6c, whose mean value is 0.0216 rad, which is the temporal phase stability of the system. This is equivalent to an optical path length stability of 2.1nm. This is also the temporal resolution of the system. This stability is considered to be good enough in application where the fluctuation of the test specimens are in the order of few tens of nanometers or higher.

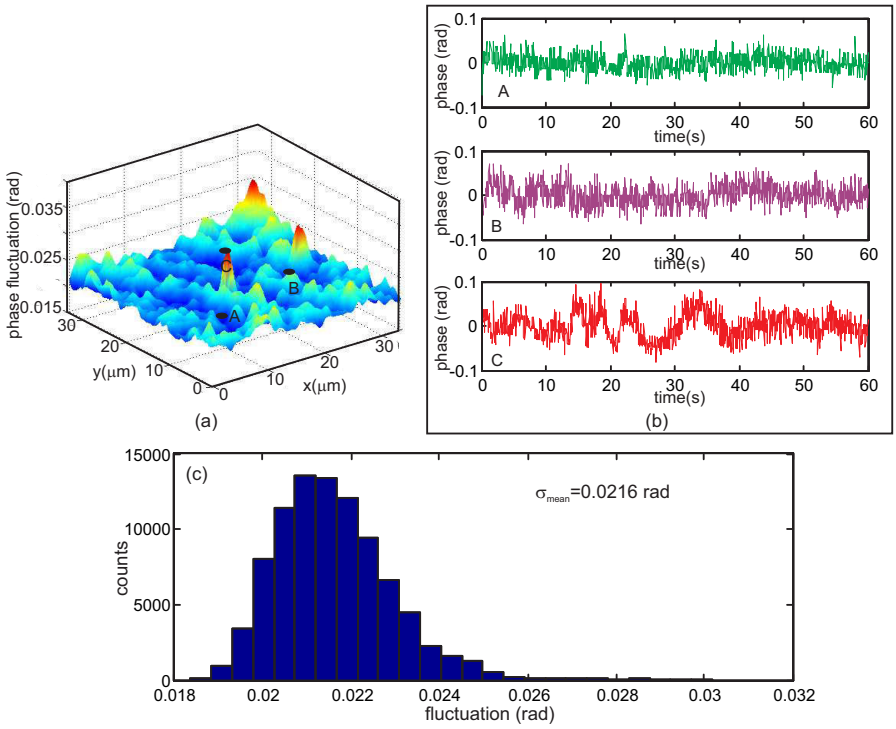

Figure 3.6: Temporal phase stability. (a) Phase fluctuation profile for an area of 300×300 pixels. (b) temporal evolution of phase along the different spatial points shown in Fig.3.6a. (c) Histogram of the phase fluctuation profile for the analyzed area.

3.6 Change in plant cell morphology with exposure

Onion cells are used as the object in the studies on plant cells using MZ-DHIM. Microscope slide are prepared with a thin single layer of onion skin cells on it. Plant cell structure varies based on its function in the plants; it contains different organelles for conduction of normal cell functions [106]. It is always important to study cell morphology and cell dynamics to understand the functioning of the cells and cell organelles under various conditions. Mach-Zehnder based DHIM is used for cellular and subcellular 3D imaging of these cells under various conditions. Onion cells (Allium Cepa) are chosen sample (Fig.3.7), as they are easily available round the year and widely used in most of the part of the world, and it has a simple and transparent cell structure presenting basic model of plant cells. Usually onion cells are $250\mu m \times 60\mu m$ in size. Holograms of these cells were recorded as a function of time and reconstructed numerically to retrieve the spatio-temporal evolution of cell morphology.

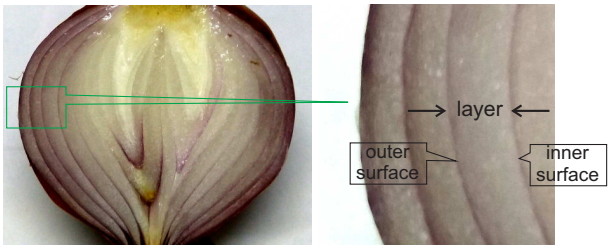

Figure 3.7: Onion layers. Image on the right shows the region inside the rectangle on the left. Inner and outer surfaces of a layer are marked.

Fig.3.8a shows a representative hologram of onion skin cells, from the inner side of a layer (see Fig.3.7) using a 20X, NA=0.4 microscope objective lens. Fig.3.8b shows the area inside the rectangle shown in Fig.3.8a. One can clearly see the high contrast interference pattern as well as the spatial modulation of the pattern due to spatial variation of cell optical thickness.

One of the advantages is the numerical focusing capability of the technique is shown in Fig.3.9. The best focus plane is determined using auto focus algorithm

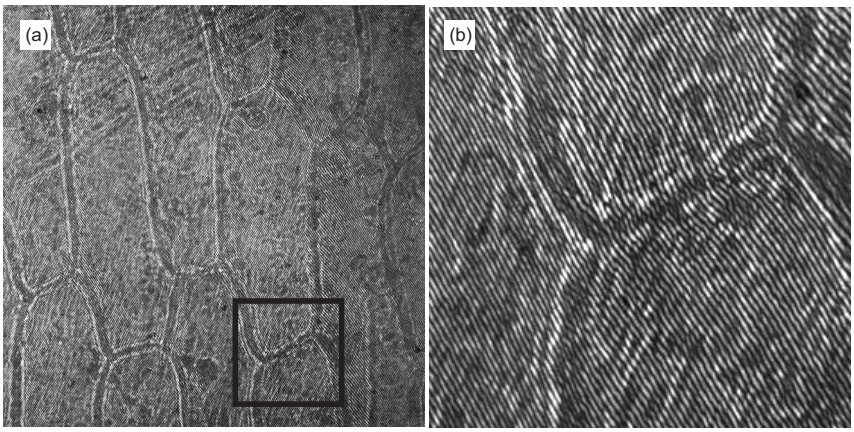

Figure 3.8: (a) Recorded digital hologram of onion cell. (b) Interference fringes inside the area of interest in Fig.3.7a.

[107]. The phase distribution at the best focus plane is used for computing thickness distribution of the cells [100].

Thin slices of the inside of onion layer on microscope slide are placed in the sample holder of the microscope to study the effect of exposure to environment on these cells. A series of holograms are recorded of at the rate of one hologram every 3 hours for the same onion cells starting from when they were fresh till 24 hours. From the reconstructed holograms, phase difference distributions are obtained. This phase information is then used to compute the optical thickness distribution of the cells. Fig.3.10a shows the obtained phase profiles (wrapped phase distribution) of onion cells just after they are mounted on the glass slide. The thickness was computed from the unwrapped phase distribution and is shown in Fig.3.10b.

Fig.3.10c and Fig.3.10d shows the quantitative phase image and the thickness profile of the cells after 24 hours. It can be seen that the volume of the cells have decreased. This is more evident from Fig.3.11, which shows the optical thickness of the cell along the line shown in Fig.3.10a.

Fig.3.12 shows the change in maximum optical thickness with time of exposure. Fig.3.10 to Fig.3.12 show that the volume (which is proportional to thickness of the cell) as well as texture of the onion skin cells changes due to exposure. Volume of the cells decreases with time, which is expected as water content reduces, which is

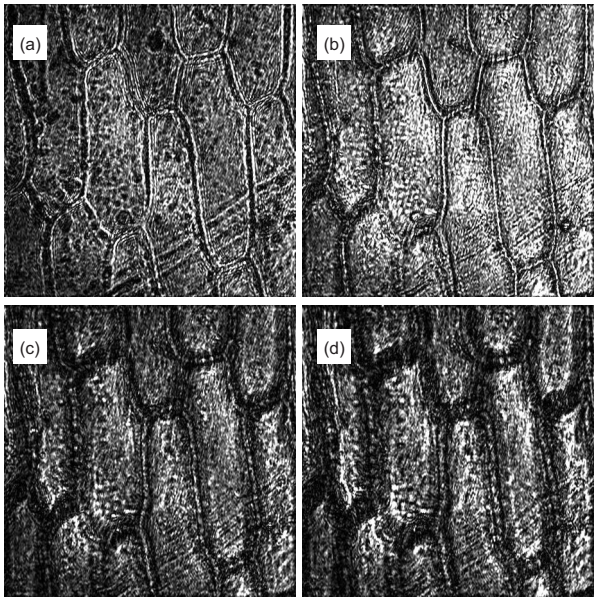

Figure 3.9: Reconstructed intensity patterns at different axial plane. (a) -28μm outside focus plane, (b) at the focus plane, (c) 15μm inside focus plane and (d) 27.5μm outside focus plane [100].

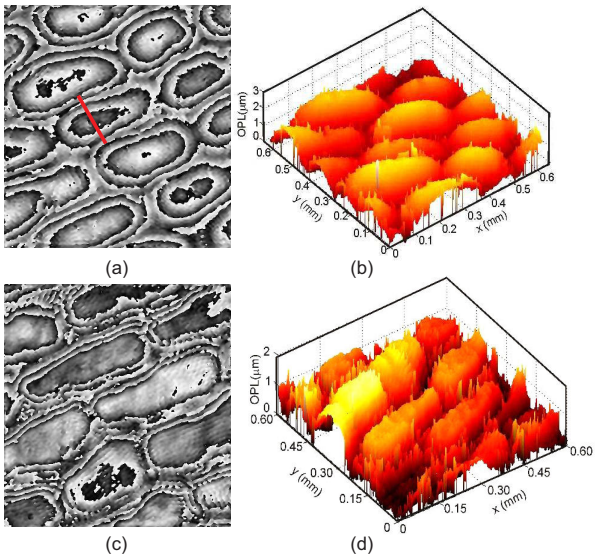

Figure 3.10: Reconstructed phase profile at the best focus plane for onion cells just after it is mounted on the glass slide. (a) Wrapped phase distribution, (b) Optical thickness distribution of the cell determined from the unwrapped phase. (c) Phase profile image after 24 hours. (d) Thickness profile after 24 hours [100].

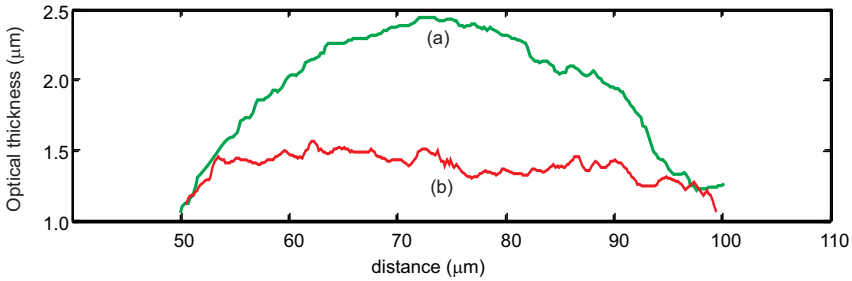

Figure 3.11: Optical thickness profile of onion skin cells. (a) Obtained optical thickness thickness profile for fresh cell. (b) Optical thickness profile after 24 hours [100].

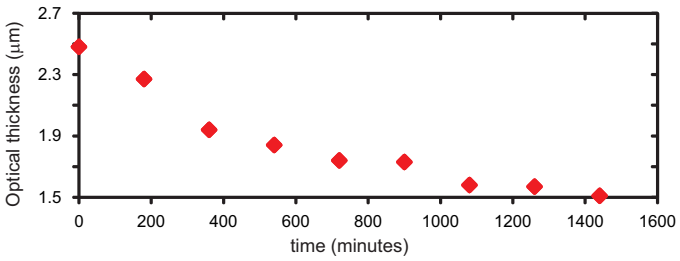

Figure 3.12: Variation in maximum optical thickness as a function of time.

due to both concentration as well as temperature gradients. The texture is found to become uneven with time (Fig.3.11b). This might be due to the cell getting dried up. The texture of the cells can be extracted after fitting the optical path length profiles with the segment averaged value, yielding the change in surface profile. The obtained optical surface roughness for freshly mounted cells was 0.42μm and this increased to 0.8μm after 24 hours, which indicates an increase in roughness of the cell membrane.

3.7 Osmosis in plant cells

Texture and crispness of fruits and vegetables is partially due to osmosis and diffusion [102]. When preservatives are applied, it creates higher ion concentration at the surface than that exists inside the cells and water permeates through the cell walls to equalize this concentration difference. So the cells lose turgor pressure (hydrostatic pressure) and begin to collapse [102]. This means that the texture of these vegetables

becomes softer and less crisp. So the effect of the effect of preservative treatment on plant cells, will lead to a change in its morphology, which could be imaged and quantified using DHIM. Change in cell morphology was studied by applying sugar solution to the onion cells.

Effect of preservatives is studied with both water externally applied to the cells (hydrostatic pressure) and sugar solution externally applied to the cells (with osmotic pressure). Fig.3.13a shows the phase images of onion cells (from the inner surface of a layer) kept between microscope slide (holograms are recorded at the rate of 15 Hz for 15 minutes) and a cover glass slide before water is introduced between the cover glass and microscope slide.

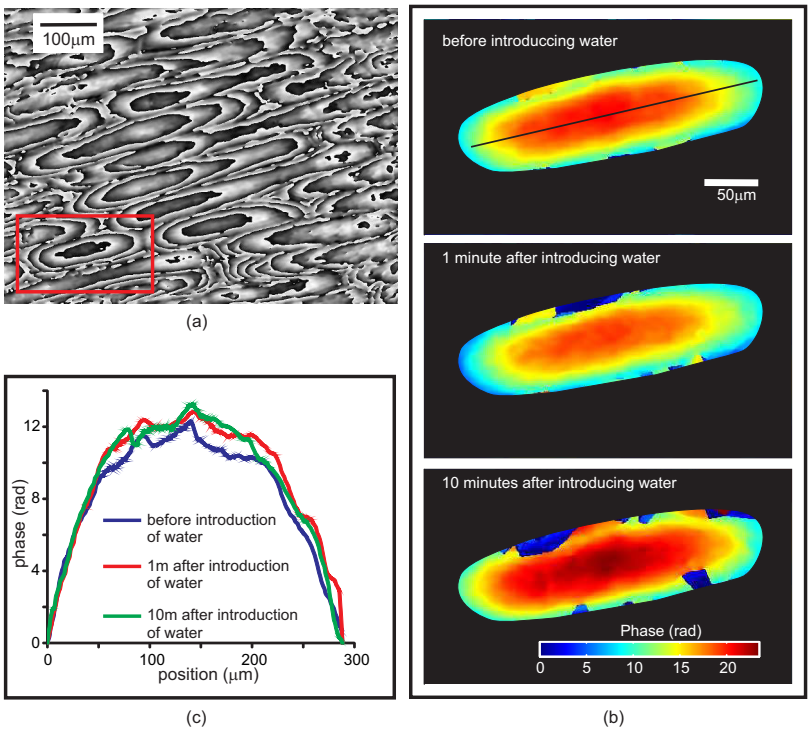

Figure 3.13: (a) Phase contrast image (unwrapped) of onion cells before introduction of water. Phase profile for the cell inside the rectangular area is used to determine effect of hydrostatic pressure on the cells. (b) Time evolution of phase inside region of interest (shown in Fig.3.13a). (c) Phase profile at different time instances (along the solid black line shown in first figure of Fig.3.13b), showing that there is only minor change in thickness of the cell even after 10 minutes of introduction of water.

Now on 100 μL of water (distilled de-ionized) is introduced between the cover slip and the microscope slide and is allowed to spread into the sample and phase profile is reconstructed (Fig.3.13b). From this figure it can be seen that the shape and the thickness of the cells remain almost same after application of water on the cells. With time a slight increase in the thickness profile is observed (Fig.3.13c), which might be due to water seeping into the cells due to hydrostatic pressure.

To see the effect of osmotic pressure on cell membrane, experiments are done with sugar solution (Sugar, NaCl, Vinegar etc. are usually used as food preservatives). Sugar solution (20mg of sugar in 100ml distilled de-ionized water) is applied to the cells and a sequence of holograms is recorded (at the rate of 15Hz). Fig.3.14 shows the reconstructed intensity profile (same as that obtained using a bright field microscope) of the cells at several instances of time. The movement of the sugar solution into onion cells can be seen (the flow front of the solution is represented by white dashed lines).

Information about what happens to cell morphology is not evident from the intensity profile (Fig.3.14). But fortunately, reconstructed holograms also provide the quantitative phase profiles, which is proportional to the thickness of the cells. This can shed light on the morphological changes occurring to the cells. Fig.3.15 shows the time variation of the phase profile for the cell inside the green rectangle shown in the first figure of Fig.3.14. Here the flow front of the sugar solution is marked by red dashed lines.

From Fig.3.15, it can be seen that as the sugar solution comes into contact with the cell, due to osmosis, due to osmosis water come out of the cells to balance the concentration gradient, thereby reducing the optical thickness of the cells. This is more evident from the cross-sectional thickness profile (along the black solid line in the first phase profile shown in Fig.3.15), which is shown in Fig.3.16, which compares the profiles before the application of sugar solution and just after the cell is immersed in the solution. These profiles were spatially averaged to obtain the smooth phase variation (shown in Fig.3.16). Fig.3.15 and Fig.3.16 together shows that the cells loose most of its contents under osmotic pressure and almost flattens out after the application of sugar solution.

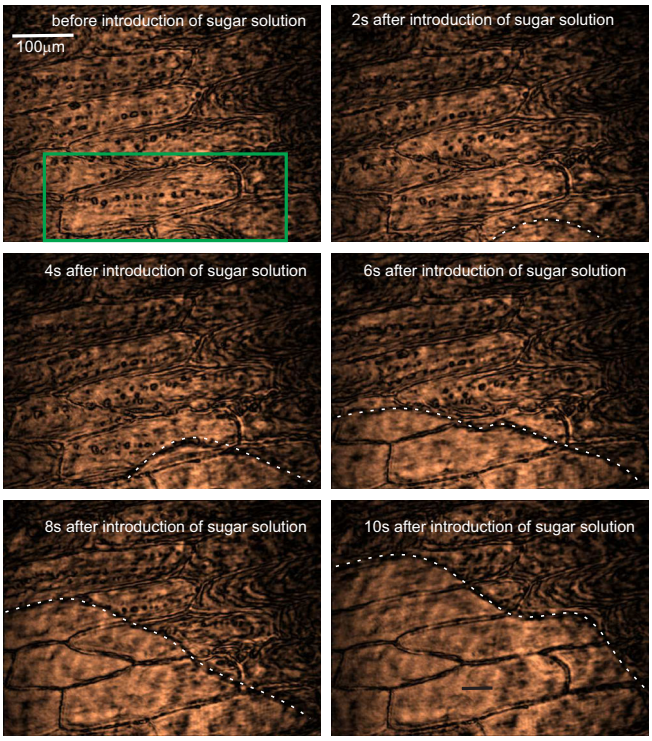

Figure 3.14: Intensity profile of the cells at different time instances as the sugar solution was spreading into the cells. Phase profile of the cell inside the green rectangle in the first figure is used to find the effect of osmotic pressure on the cells. Flow front of sugar solution is shown as white dashed line.

3.8 Cell morphology dependence on germination

Onion bulb contains layers of fleshy scale leaves which function as food storage organ, each covered with inner and outer epidermis (Fig.3.7). The cells on the outer surface contain less amount of water compared to that at the inner surface.

Fig.3.17a and Fig.3.17b shows the unwrapped quantitative phase image as well as the three dimensional rendering of the optical thickness profile for cells on the outer surface of a layer. Visually, unwrapped phase profile provides a better insight into the thickness of the cell with each change from a white to black or black to white phase region representing a thickness change equivalent to one λ (vacuum wavelength of the laser source). Compare this to the phase profile and thickness distribution shown in Fig.3.17c and Fig.3.17d respectively for cell from the inner surface of the layer. In

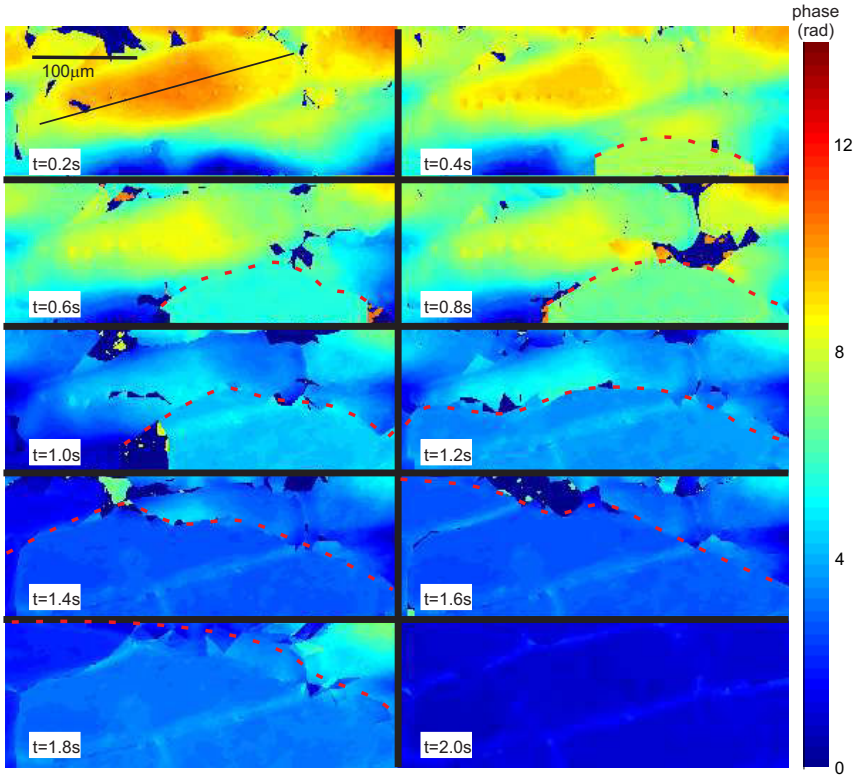

Figure 3.15: Quantitative phase profile of the cells as a function of time. As the sugar solution comes into contact with the cell, its thickness drastically decreases.

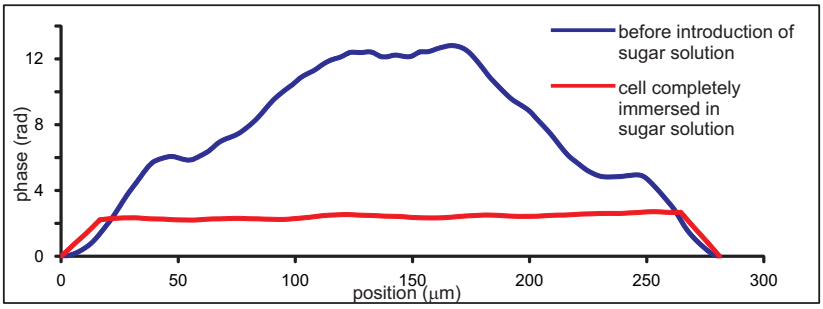

Figure 3.16: Cross-sectional phase profiles at different time instances (along the solid black line shown in first phase image in Fig.3.15), showing that the cell almost flattens after it is completely immersed in sugar solution due to osmotic pressure.

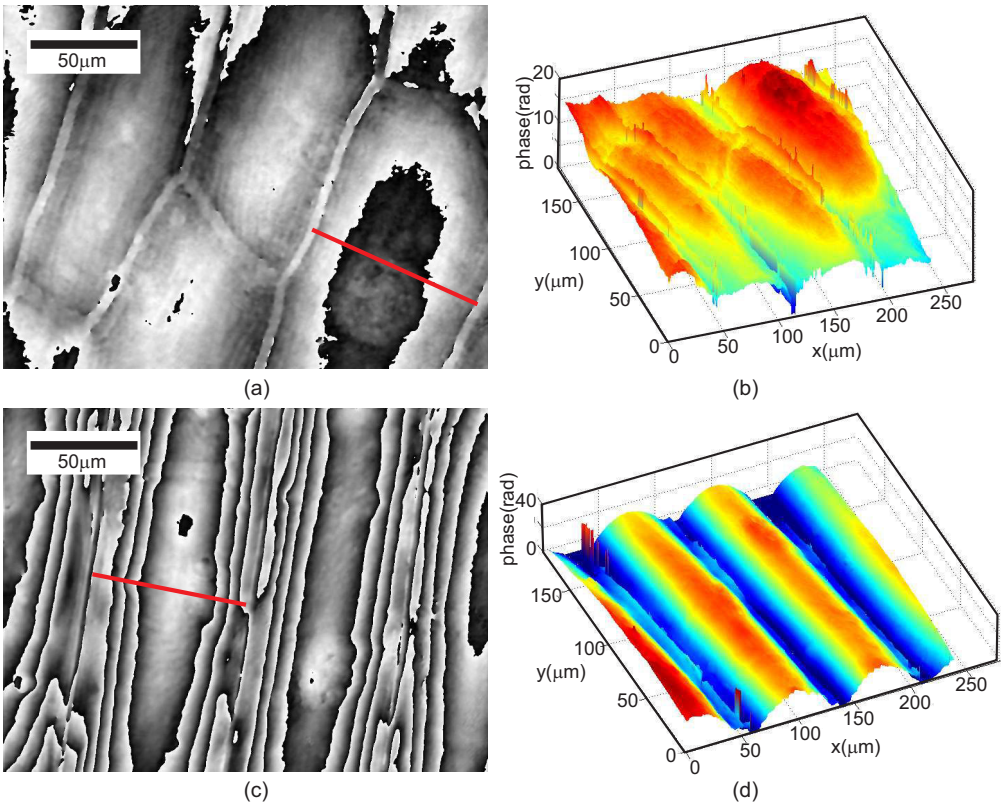

Figure 3.17: Quantitative phase contrast images of un-germinated onion cells, (a) outer surface and (c) inner surface. Thickness profile distribution of these cells are shown in (b) for outer surface and (d) for inner surface. Phase profile along the solid red line in (a) and (c) are compared to estimate the effect of germination on cells.

onion bulb inner epidermis (inner surface) is usually thicker than the outer epidermis and that this can be seen and from Fig.3.17. Similar results (thickness of cells on the inner surface is greater than thickness of cells on the outer surface) were obtained for almost all of the cases.

Onion is then germinated by keeping it with the root end down in a transparent glass filled with water to cover the roots of onion bulb. This is kept for two days and new root growth is observed. Microscope slides are then prepared using thin slices of inner and outer epidermis (inner and outer surface) of a scale leave from this germinated bulb. Fig.3.18 shows effect of germination on the cell morphology.

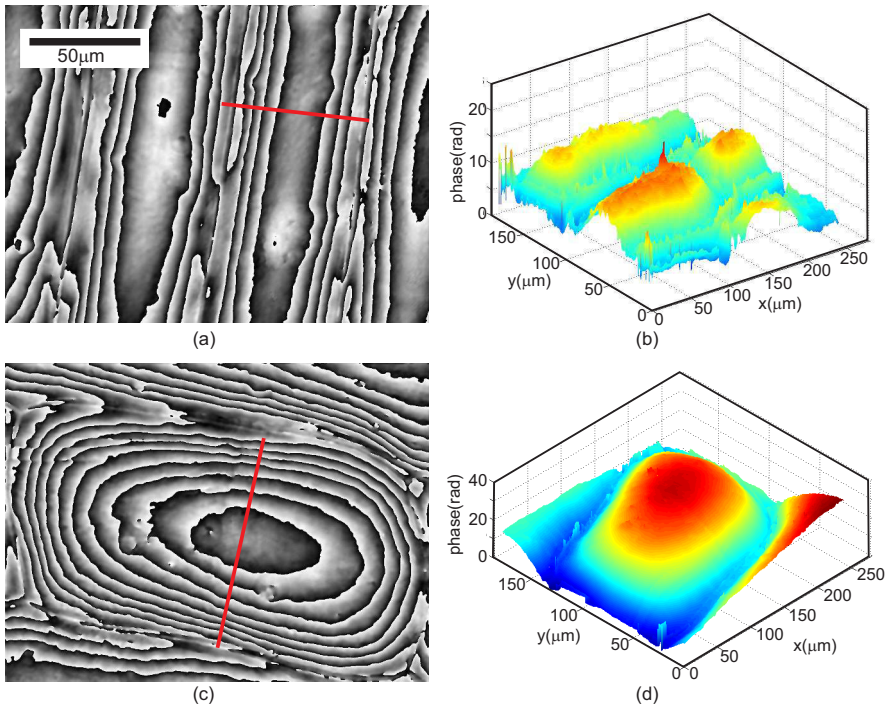

Figure 3.18: Quantitative phase contrast images in the case of germinated onion cells, (a) cells of outer surface and (c) cells on the inner surface. (b) Thickness profile of cells in outer surface and (d) Thickness profile of cells on inner surface. Phase profile along the solid red line in (a) and (c) are compared to estimate the effect of germination on cells.

Comparing the thickness profiles for non-germinated onion cells (Fig.3.17) and

germinated onion cells (Fig.3.18), it is seen that cells on both inner and outer epidermis layers grow thicker on germination, with the cells on inner layer growing more. This comparison is of thickness profiles are shown in Fig.3.19 along the solid red line shown in Fig.3.17 and Fig.3.18 (unwrapped phase distribution).

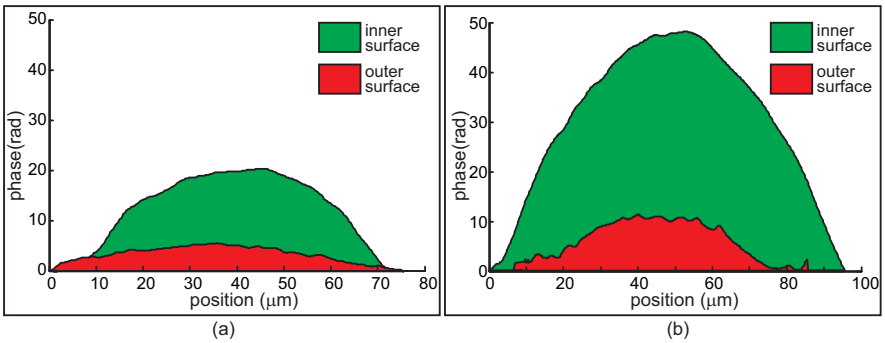

Figure 3.19: Cross-sectional of thickness profile. (a) Before germination. (b) After germination

Cells of germinated onions are thicker because of increase of water absorbed by roots. This basic comparative study may lead the intensive study of germination process in different plant seeds.

3.9 Study of sub-cellular structures of plant cells

Plant cells contain subcellular components or organelles for conducting various functions. These include the nucleus, cell wall, stomata etc. These components can be quantified using MZ-DHIM.

The nucleus is the organelle that contains the genetic information primarily responsible for regulating the cell's activities such as metabolism, growth, and differentiation of the cell. It is surrounded by nuclear membranes [106]. Fig.3.20a shows the hologram of onion cells and Fig.3.20b is the portion inside the blue rectangle showing the fringe modulation in the regions of the nucleus and cell wall.

In the quantitative phase image of the onion skin cells nucleus inside can be clearly seen without any labelling (Fig.3.20a). By the use of global thresholding of the phase image with the background phase (which is the average of the phase values/thickness

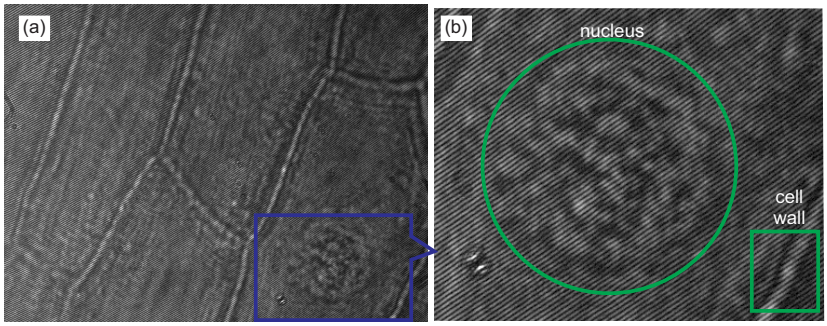

Figure 3.20: (a) hologram of onion cells showing the region of nucleus. (b) Region inside the blue rectangle showing the modulation of the interference fringes in the region of the nucleus as well as at the cell walls.

values just around the nucleus - shaded area surrounding the nucleus in Fig.3.20a), the phase profile of the nucleus alone can be extracted (Fig.3.20b). Three dimensional the thickness profile of the entire cell nucleus as well as its cross sectional thickness profile are shown in Fig.3.21c and Fig.3.21d respectively. Since the location as well as the projection on the thickness profile on a plane are available, the size, area and volume (optical) of the cell as well as the nucleus become measurable.

Most plant cells are surrounded completely by cell wall. It gives shape to the cells, protecting it against mechanical stress. It also controls molecules entering or leaving. In cell differentiation and water movement in the cells it plays a key role. Composition and properties of cell wall varies with cell type, and may get changed with development process of the cells. To compare and analyze wall structure of different cells of various plants, vegetables or fruits, MZDHM can be used. Fig.3.22 shows quantitative imaging of walls of onion cells. Fig.3.22a shows the phase distribution around the wall of a cell on the outer surface of a layer (Fig.3.7) and the corresponding 3D image is shown in Fig.3.22c. Phase distribution and 3D image of cell wall for inner surface is shown in Fig.3.22b and Fig.3.22d respectively.

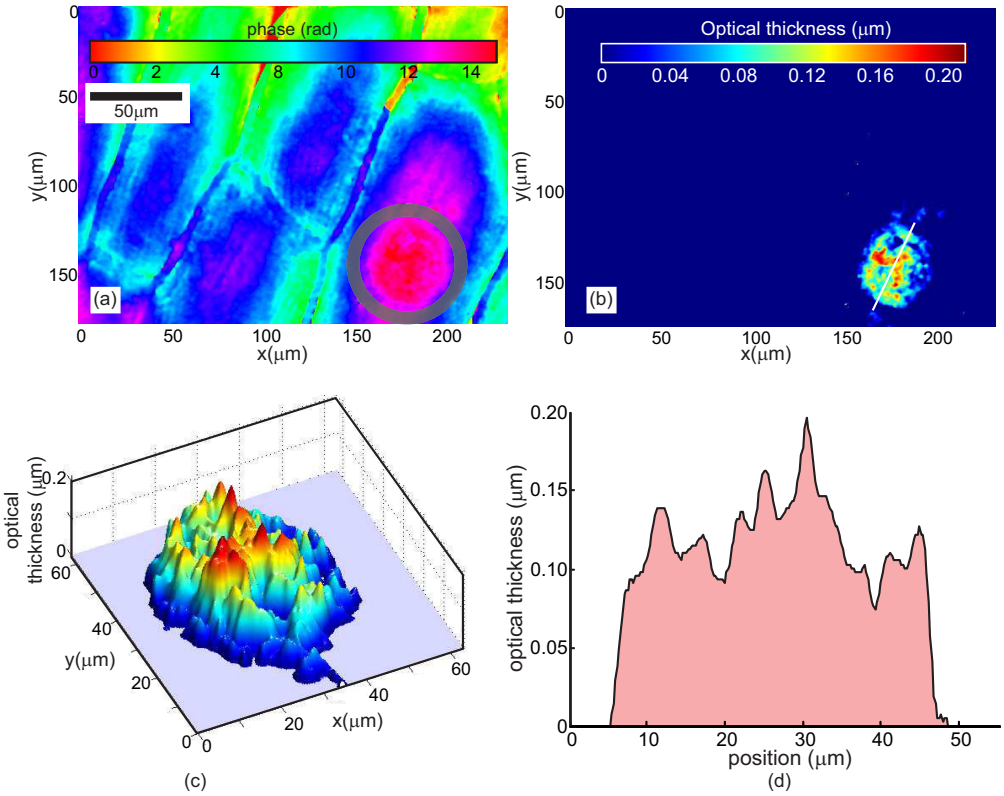

Figure 3.21: (a) Quantitative phase image (unwrapped) of the onion cell, with the cell nucleus visible. (b) Optical thickness profile of the cell nucleus obtained after global thresholding of the thickness profile by the average of the phase value just around the cell nucleus (shaded ring shaped region in Fig.3.21a). (c) Three dimensional rendering of the optical thickness profile of the cell nucleus. (d) Cross sectional thickness profile along the line in Fig.3.21b.

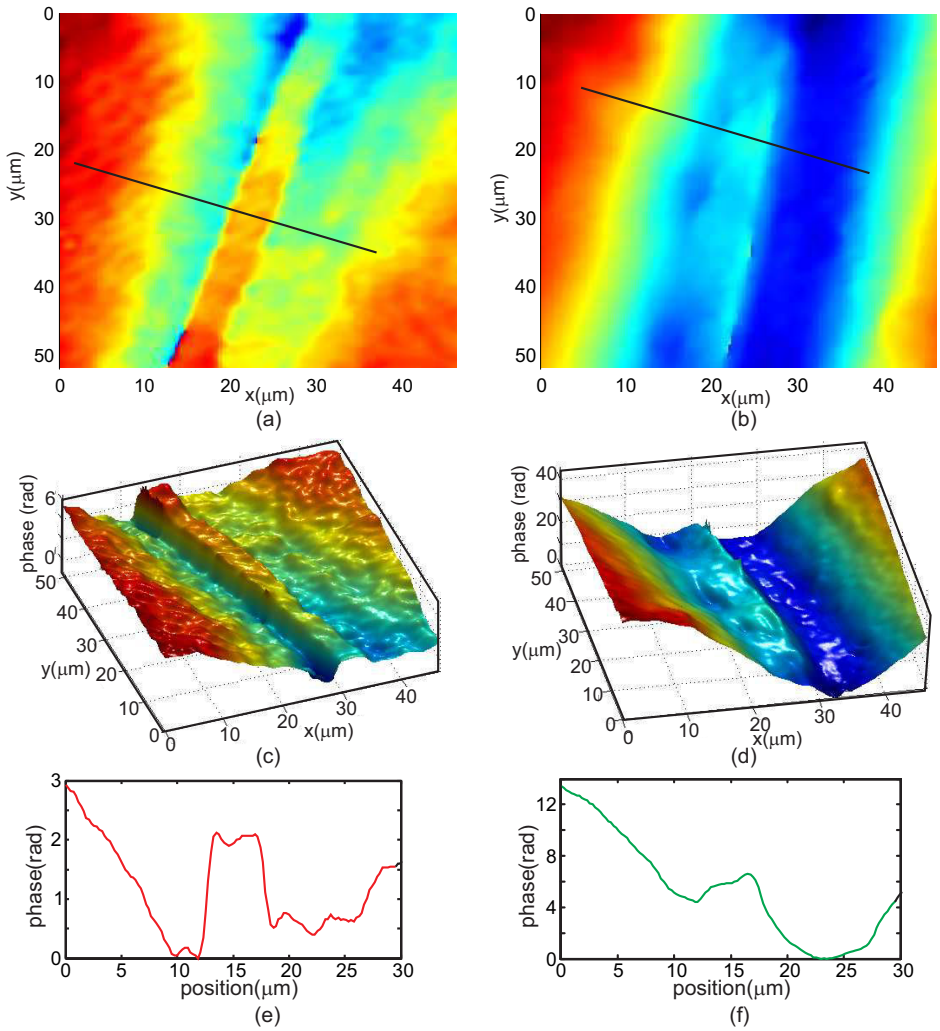

Figure 3.22: (a) Quantitative phase image (unwrapped) of the wall of onion cells from the outer surface of a layer and (c) 3D profile of the cell wall. (b) Phase image of the wall of onion cells from the inner surface of a layer and (d) three dimensional rendering of the phase profile of the wall. (e) and (f) represents the cross sectional phase profile of the cells from the outer and inner surfaces respectively, along the lines shown in Fig.3.22a and Fig.3.22b.

3.10 Conclusions

MZ-DHIM is demonstrated for its application in imaging of planet cells. Since this imaging modality provides direct accesses to thickness information of cells, many parameters of the cell, which depends upon its thickness can be quantified and studies. Different properties of the cells such as its change in morphology due to exposure to atmosphere, effect of osmosis on the structure and shape of the cells, cell shape dependence on germination were studied. Results are compared for fresh and dry cells of onion, for cells from various layers of onion bulb, for cells from germinated and normal cells and also for the cells before and after applying preservative solution. Holograms of subcellular organelles like nucleus and cell walls were reconstructed to see their 3D structure and optical thickness. Summarizing this chapter, it is important to emphasize that the Mach-Zehnder Digital Holographic Microscope, an off-axis configuration that makes numerical reconstruction easy as it removes the twin image problem was applied to study plant cells. This experimental study of plant cells and subcellular parts is an attempt to show importance of the technique in botanical sciences, agriculture, and biotechnology and also in food processing.